SUPPLEMENTARY INFORMATION

Creating Capsules with Cubanes

Sotaro Kusumoto, Fumiya Kobayashi, Ryo Ohtani, Yingjie Zhang, Jack Harrowfield, Yang Kim,

Shinya Hayami*, Masaaki Nakamura*

1. Synthesis of ligands and complexes

2. Physical measurements

3. Crystallographic data

**4. Infra-red spectra**

5. PXRD patterns

6. Magnetic susceptibility

7. TGA measurements

1. Synthesis of ligands and complexes

All reagents and solvents used in the syntheses, obtained from Tokyo Kasei Co. and Wako Pure Chemical Industries, were of reagent grade and used without further purification. All reactions were carried out in air. H**L¹** was synthesized by a literature procedure[1] and H**L²** by the same procedure modified by the substitution of 1,5-diaminopentane for 1,3-diaminopropane as described below. Elemental analyses (C,H,N) were carried out on a J-SCIENCE LAB JM10 analyzer at the Instrumental Analysis Centre of Kumamoto University.

Synthetic scheme of H**L¹** and H**L².**
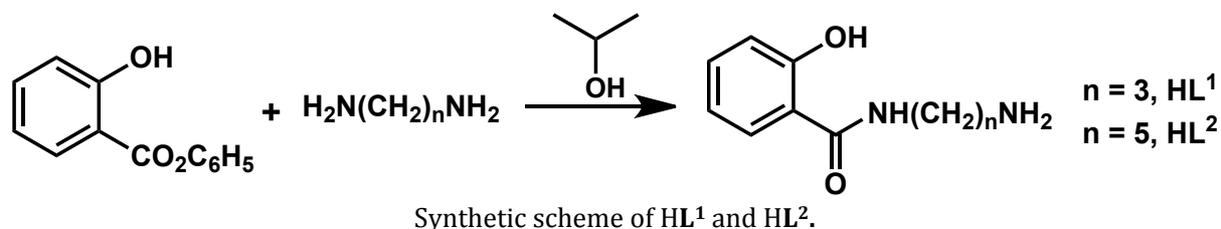
N-(5-aminopropyl)-2-hydroxy-benzamide (HL²)

Phenyl salicylate (2.133 g, 10 mmol) in 2-propanol (80 mL) was added dropwise, with stirring, over 1 h to a solution of 1, 5–diaminopentane (0.102 g, 10 mmol) in 2-propanol. Stirring was then continued for two days at room temperature. The white precipitate formed was collected by filtration, washed with 2-propanol and dried *in vacuo*. Yield: 1.23 g (55%). ^{1}H NMR (500 MHz, DMSO-d_6): δ 1.33 (quint, 2H, CH_2-CH_2-CH_2), 2.66 (t, 2H, CH_2NH$_2$), 3.35 (s, 2H, NH-CH_2), 6.64 (f, 1H, C(5)H), 6.75 (d, 1H, C(3)H), 7.22 (d, 1H, C(4)H), 7.75 (d, 1H, C(6)H). ^{13}C NMR (DMSO-d_6, 125 MHz): δ 168.4, 163.7, 132.7, 128.7, 118.7, 117.2, 115.4, 40.42, 38.49, 30.64, 29.17, 23.80. Major IR absorptions: 2937, 1550, 1441, 1333, 1137, 772 cm^{-1}.
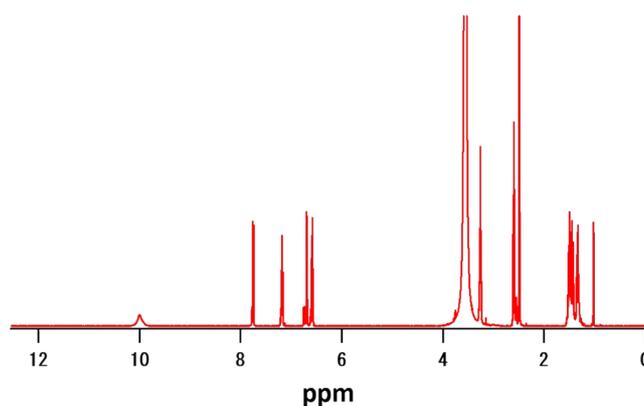
^{1}H NMR spectrum of H**L²** in DMSO-d^6.

[Ni₈(L¹)₆(μ₃–OCH₃)₆(CH₃OH)₆(μ₃–Cl)(μ₃–OCH₃)]Cl₂·9H₂O (1)

H**L¹** (0.116 g, 0.6 mmol) and triethylamine (0.05 g, 0.5 mmol) were dissolved in methanol (30 mL) then mixed with a methanol solution (30 mL) of NiCl$_2$·6H$_2$O (0.190 g, 0.8 mmol). The mixture was stored for several weeks in a closed vessel, resulting in formation of blue-green, block-shaped crystals. These were collected by filtration, washed with methanol and dried *in vacuo*. Yield: 0.12 g (55%) Anal. Found: C, 37.89; H, 5.53; N, 7.62 %. Calcd for [Ni₈(**L¹**)₆(μ₃–OCH₃)₆(CH₃OH)₆(μ₃–Cl)(μ₃–OCH₃)]Cl₂·9H₂O (C₇₃H₁₄₁Cl₃N₁₂Ni₈O₃₄): C, 38.01; H, 6.16; N, 7.29 %. Major IR absorptions: 2933, 1600, 1527, 1447, 1335, 1231, 1143, 1028 cm^{-1}.

[Ni₈(L²)₆(μ₃–OCH₃)₆(OH₂)₆(μ₃–OH)₂](BF₄)₂·4H₂O (2)

H**L²** (0.13 g, 0.6 mmol), sodium tetrafluoroborate (0.054 g, 0.5 mmol) and trimethylamine (0.05 g, 0.5 mmol) were dissolved in methanol (30 mL), then slowly added to a methanol solution (30 mL) of

NiCl$_2$·6H$_2$O (0.190 g, 0.8 mmol). The mixture was allowed to stand for two weeks in a closed vessel, resulting in formation of blue-green block-shaped crystals. These were collected by filtration, washed with methanol and dried *in vacuo*. Yield: 0.074 g (28%). Anal. Found: C, 39.63; H, 6.38; N, 7.15 %. Calcd for [Ni$_8$(**L^2**)$_6$(μ_3–OMe)$_6$(OH$_2$)$_6$(μ_3–OH)$_2$](BF$_4$)$_2$·4H$_2$O (C$_{78}$H$_{142}$B$_2$F$_8$N$_{12}$Ni$_8$O$_{30}$): C, 39.50; H, 6.03; N, 7.09 %. Major IR absorptions: 2940, 1600, 1530, 1340, 1040 cm^{-1}.

[Ni$_8$(L^2)$_6$(μ_3–OCH$_3$)$_6$(CH$_3$OH)$_6$(μ_3–OH)$_2$](ClO$_4$)$_2$·11H$_2$O (3)

H**L^2** (0.13 g, 0.6 mmol), sodium perchlorate (0.061 g, 0.5 mmol) and triethylamine (0.05 g, 0.5 mmol) were dissolved in methanol (30 mL). The methanol solution was slowly add to a methanol solution (30 mL) of NiCl$_2$·6H$_2$O (0.190 g, 0.8 mmol). The mixture was allowed to stand for a week in a closed vessel, resulting in formation of blue-green block-shaped crystals. These were collected by filtration, washed with methanol and dried *in vacuo*. Yield: 0.062 g (29%). Anal. Found: C, 38.56; H, 6.22; N, 6.90 %. Calcd for [Ni$_8$(**L^2**)$_6$(μ_3–OMe)$_6$(CH$_3$OH)$_6$(μ_3–OH)$_2$](ClO$_4$)$_2$·11H$_2$O (C$_{84}$H$_{178}$Cl$_2$N$_{12}$Ni$_8$O$_{45}$): C, 38.70; H, 6.50; N, 6.45 %. Major IR absorptions: 2940, 1610, 1530, 1340, 1059 cm^{-1}.

*Note that crystals of all the complexes effloresced quite rapidly on exposure to the atmosphere and those used for the structure determinations were taken directly from the reaction mixtures and mounted without drying.

2. Physical measurements

Infrared (IR) spectra measurements were performed on a PerkinElmer Spectrum Two FT-IR equipped with an ATR accessory. Temperature-dependent magnetic susceptibilities between 2 K and 300 K were measured by using a superconducting quantum interference device (SQUID) magnetometer (Quantum Design MPMS XL) in an external field of 0.5 Oe. The magnetic susceptibility data were fitted using the program PHI.[5] Elemental analyses (C,H,N) were carried out on a J-SCIENCE LAB JM10 analyzer at the Instrumental Analysis Centre of Kumamoto University. Thermogravimetric analysis (TGA) was performed at 10 K min^{-1} using a Rigaku Instrument Thermo plus TG 8120 in a nitrogen atmosphere. Powder X-ray diffraction data (PXRD) were collected on a RIGAKU MiniFlex II ultra (30 kV/15 mA) X-ray diffractometer using Cu K_α radiation (λ = 1.5406 Å) in the 2ϑ range of 2°−30° with a step width of 1.0°.

3. Crystallographic data

X-ray diffraction data for the single crystal **1** were collected with a Rigaku XtaLAB mini II diffractometer. The structures were solved by direct methods (SHELXT) and refined by full-matrix least-squares refinement using the SHELXL computer program. Hydrogen atoms were refined geometrically using a riding model. The single crystal X-ray diffraction measurements for **2** and **3** were carried out on the MX1 beamline at the Australian Synchrotron. Diffraction data were collected using Si<111> monochromated synchrotron X-ray radiation (λ = 0.71074) at 100(2) K with BlueIce software[1] and were corrected for Lorentz and polarisation effects using the XDS software.[2] The structure was solved with SHELXT[3] and the full-matrix leastsquares refinements were carried out using SHELXL-2014 via the Olex2 interface.[4] All non-hydrogen atoms with occupancies over 0.5 were located from the electron density maps and refined anisotropically. Hydrogen atoms bound to carbon, nitrogen and oxygen atoms were added in the ideal positions and refined using a riding model.

Table S1. Crystallographic data for complexes **1-3**.

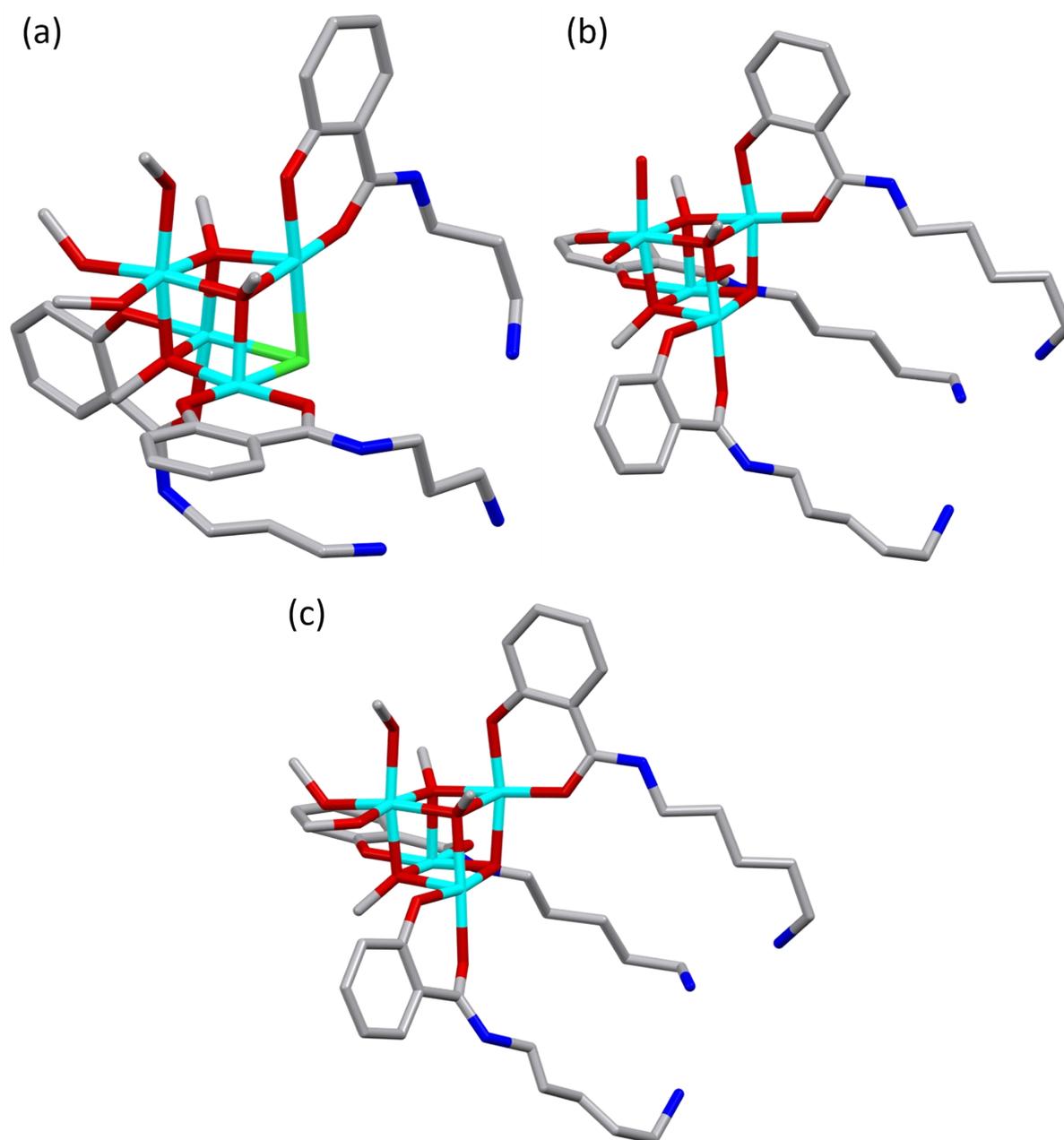| Compound	1	2	3
formula	$C_{79}H_{147}Cl_3N_{12}Ni_8O_{31}$	$C_{78}H_{132}BF_4N_{12}Ni_8O_{26}$	$C_{89}H_{157}Cl_2N_{12}Ni_8O_{36.75}$
formula weight	2337.05	2210.29	2523.84
crystal system	triclinic	monoclinic	triclinic
space group	$P-1$	$P2_1/c$	$P-1$
a / Å	14.1511(10)	21.433(4)	15.900(3)
b / Å	14.1612(13)	22.146(4)	17.230(3)
c / Å	16.7040(12)	35.041(7)	21.830(4)
α / º	65.340(8)	90	91.79(3)
β / º	66.649(7)	103.89(3)	92.92(3)
γ / º	61.292(8)	90	90.57(3)
V / Å³	2586.3(4)	16146(6)	5969(2)
Z	1	6	2
T / K	150 K	100 K	100 K
R_1	0.0467	0.1004	0.0788
wR_2	0.1405	0.3296	0.2140
G.O.F.	1.070	1.007	1.096

(a)

(b)

(c)

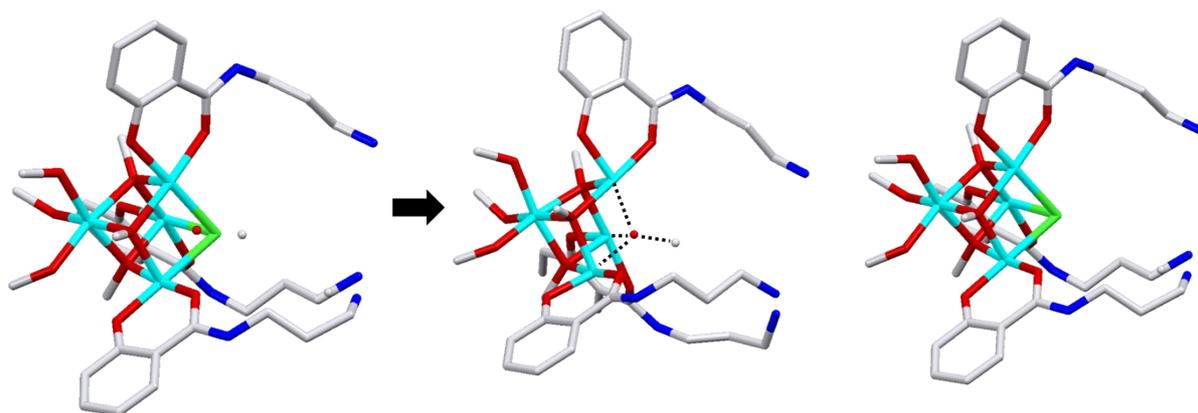Figure S1. Half dicubane units of a molecule (a) **1**, (b) **2**, (c) **3**.

Figure S2 Disordered model of **1**. The μ^3-Cl bridge and the μ^3-OCH$_3$ bridge at 1:1 ratio in the crystal. The refined occupancies of the Cl1 and C16-O40 atom are 0.5, respectively.
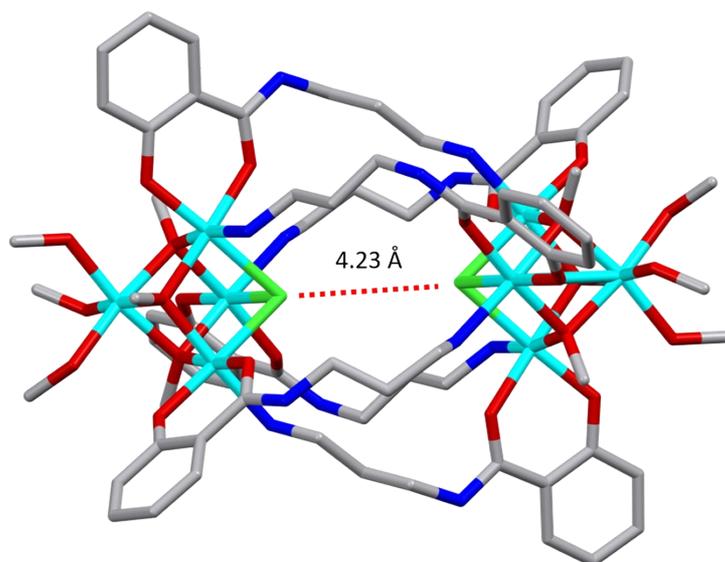
Figure S3. Cl···Cl separations (red dashed lines) of **1**.
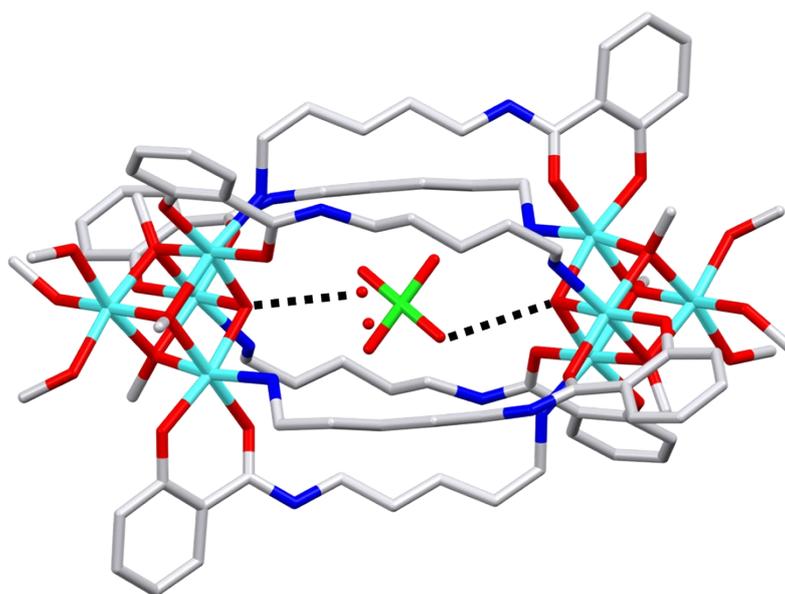

Figure S4.   O···O contacts (black dashed lines) taken to be indicative of H-bonding interactions of the included anion in one of the capsular units present in the lattice of **3**.

Structure refinements

In general, non-hydrogen atoms with occupancies over 0.5 were located from the electron density maps and refined anisotropically. Hydrogen atoms bound to carbon, nitrogen and oxygen atoms were added in the ideal positions and refined using a riding model. Hydrogen atoms on crystalline water or ethanol molecules are generally omitted in the final structure refinements due to the extensive disorders. One BF_4^- inside the cage is also disordered in complex **2**. All ClO_4^- anions are disordered either inside the cages or in the crystal lattice in complex **3**.
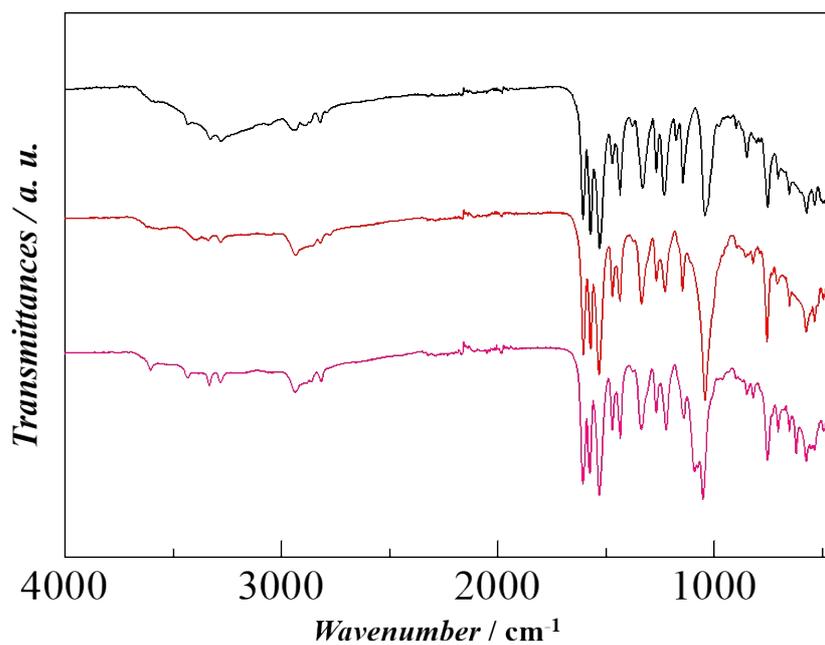
4. Infra-red spectra

Figure S5. IR spectra of the **L²** complexes. **1** (black), **2** (red), **3** (pink).
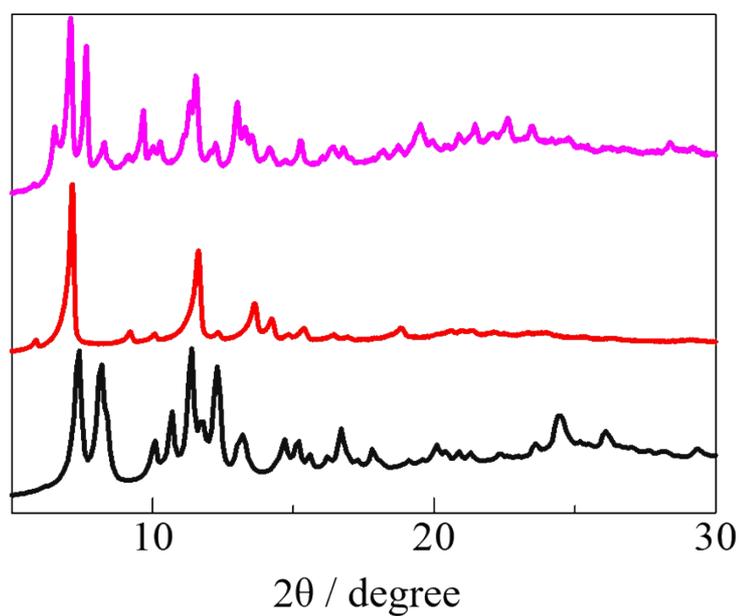
5. PXRD patterns

Figure S6. PXRD patterns of the **L²** complexes. **1** (black), **2** (red), **3** (pink).

6. Magnetic susceptibility

All measurements were made on powdered samples in a 5000 Oe field using a SQUID. Red triangles are experimental points and the blue lines are the curves obtained from the fit to the Hamiltonian $H = -2J_1(S_2S_3+S_1S_3+S_3S_4)-2J_2(S_1S_4+S_2S_4+S_1S_2)$ for the model given in the main text.

Table S2. Best Fit Parameters of Magnetic Data for Complexes **1**–**3**.

Complex	g	J_1 [cm^{-1}]	J_2 [cm^{-1}]	$R*$
1	2.29	+5.71	+0.92	1.67×10^{-5}
2	2.34	+3.15	+3.15	2.30×10^{-5}
3	2.33	+6.67	+1.88	2.23×10^{-7}

$*R = \Sigma(\chi_mT_{exp}-\chi_mT_{calc})^2/\Sigma(\chi_mT_{exp})^2]$

7. TGA measurements

(a)   (b)   (c)
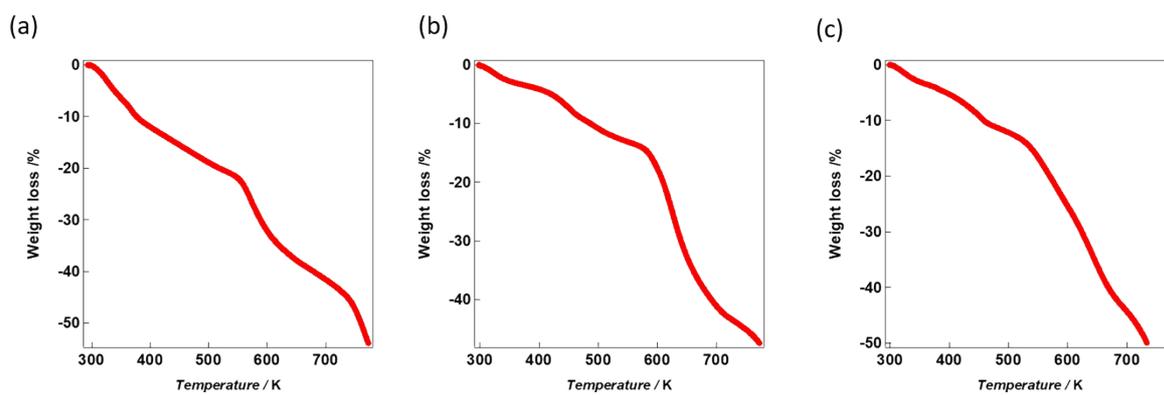
Figure S7. TGA results for powder samples of (a) **1,** (b) **2,** (c) **3**.

References

1. (a) R. Mitsuhashi, T. Suzuki, Y. Sunatsuki, M. Kojima., *Inorg. Chim. Acta,* 2013, **399**, 131–137. (b) J. −P. Costes, F. Dahan, B. Donnadieu, M. −J. R. Douton, M. −I. F. Garcia, A. Bousseksou, and J. −P. Tuchagues, *Inorg. Chem.*, 2004, **43**, 2736–2744.
2. T. M. McPhillips, S. E. McPhillips, H. J. Chiu, A. E. Cohen, A. M. Deacon, P. J. Ellis, E. Garman, A. Gonzalez, N. K. Sauter, R. P. Phizackerley, S. M. Soltis, P. Kuhn, *J. Synchrotoron Radiat*. 2002, **9**, 401-406.
3. W. Kabsch, *J. Appl. Cryst*. 1993, **26**, 795-800.
4. (a) G. M. Sheldrick, *Acta Cryst.* 2015, **C71***,* 3-8; (b) G. M. Sheldrick, *SHELXL-2014,* University of Göttingen, 2014.
5. O. V. Dolomanov, L. J. Bourhis, R. J. Gildea, J. A. K. Howard, H. Puschmann, *J. Appl. Cryst.* 2009, **42**, 339-341.
6. N. F. Chilton, R. P. Anderson, L. D. Turner, A. Soncini, K. S. Murray, *J. Comput. Chem*. 2013, **34***,* 1164-1175.